Characterisation of fatigue damage in composites using an Acoustic Emission Parameter Correction Technique

Safaa Kh Al-Jumaili, Mark J. Eaton, Karen M. Holford, Matthew R. Pearson, Davide Crivelli, Rhys Pullin

PII: S1359-8368(17)31006-5

DOI: 10.1016/j.compositesb.2018.06.020

Reference: JCOMB 5750

To appear in: *Composites Part B*

Received Date: 21 March 2017

Revised Date: 1 May 2018

Accepted Date: 16 June 2018

Please cite this article as: Al-Jumaili SK, Eaton MJ, Holford KM, Pearson MR, Crivelli D, Pullin R, Characterisation of fatigue damage in composites using an Acoustic Emission Parameter Correction Technique, *Composites Part B* (2018), doi: 10.1016/j.compositesb.2018.06.020.

Characterisation of Fatigue Damage in Composites Using an Acoustic Emission Parameter Correction Technique

Safaa Kh Al-Jumaili[a, b], Mark J Eaton[a], Karen M Holford[a], Matthew R Pearson[a], Davide Crivelli[a] and Rhys Pullin[a]

[a] Cardiff School of Engineering, Cardiff University, Queen's buildings, The Parade, Cardiff, CF24 3AA, UK
[b] University of Basrah, Engineering College, Materials Engineering Department, Basrah, Iraq
E-mail addresses: SafaaKh@gmail.com (Safaa Kh. Al-Jumaili), EatonM@cardiff.ac.uk (Mark J. Eaton), Holford@cardiff.ac.uk (Karen M. Holford), pearsonmr@cardiff.ac.uk (Matthew R. Pearson), crivellid@cardiff.ac.uk (Davide Crivelli) and PullinR@cardiff.ac.uk (R. Pullin).
Corresponding author: Safaa Kh. Al-Jumaili, University of Basrah, Engineering College, Materials Engineering Department, Basrah, Iraq
Email: SafaaKh@gmail.com, Tel. : +9647733974565

Abstract

In industrial applications of composite materials, accurate characterisation of damage is vital. Acoustic Emission (AE) can be utilised to achieve this, however, in large-scale complex geometry components, traditional AE approaches have limitations. In this study a large carbon fibre specimen was used to generate different damage mechanisms under fatigue loading. The Delta T Mapping technique was used to locate damage and signal features were corrected using the Parameter Correction Technique (PCT). A comparison between results obtained using traditional signal features and those obtained using PCT is given. The results are validated using C-scanning and computed tomography. Matrix cracking and delamination were successfully identified using the PCT approach and improved location accuracy was achieved.

Keywords: A. Carbon fibre; D. Acoustic emission; Damage characterisation; Damage location

1. Introduction

Fibre reinforced composite materials are extensively used in large-scale applications for infrastructure and transport, (aerospace, energy, automotive and marine), thanks to their high strength to weight ratio. As a result, there is a need to ensure that structural integrity is maintained which requires a deeper understanding of mechanical behaviour, damage mechanisms and remaining life to failure under static and fatigue load regimes. Many Non-Destructive Evaluation (NDE) techniques can contribute to this and one such technique is Acoustic Emission (AE) which is the passive monitoring of stress waves in a structure [1]. The stress waves originate in materials when strain energy is released during damage growth. If suitable sensors are used, such as piezoelectric transducers, the released energy can be detected. This feature can be usefully exploited for the real time monitoring of a structure and enables the provision of feedback about the structures integrity and damage evolution and hence can increase the time periods between inspections. This is particularly useful in order to reduce cost of inspection especially on hard to access structures such as off-shore wind turbines. Moreover, the use of AE allows the determination of damage locations within a structure and the identification of the damage mechanisms present by consideration of the detected AE signal features. This enables the AE technique to be used very effectively to investigate the integrity of composite structures [2]. Many studies have been conducted on different composite systems using the AE technique for monitoring real-time damage evolution and identifying different types of damage due to its high sensitivity to various damage modes [3, 4].

Despite some success, full-scale damage identification using AE remains a significant challenge and is a non-trivial task. Damage characterisation using AE is well established for small isotropic components where the attenuation effects are low, but the use of AE to investigate failure mechanisms in large-scale components has been limited by the effects of propagation. Furthermore, many traditional Non-Destructive Testing (NDT) techniques do not perform well in composite materials due to their anisotropic properties. Most composite materials have a distinct anisotropic mechanical behaviour which leads to complex wave propagation and scattering phenomena. Large-scale structures also often contain geometric features such as holes, curvatures and thickness changes, which further interrupt signal propagation paths. A further challenge faced in signal classification is the variation of sensor transfer function between different sensors. To eliminate these effects the best practice for signal classification is to only consider signals recorded by a single sensor. However, large structures require the use of multiple sensors to achieve full coverage and this is particularly so in composite structures where attenuation is commonly high. The variation between sensor transfer functions can therefore have a significant effect on classification accuracy.

Hence careful consideration of AE data is required in order to maximise subtle differences and increase characterisation accuracy of composite damage mechanisms. It is understood that even in a similar test with permanent test conditions each sensor can record different AE signals due to sensor characteristics, sensor location, signal attenuation and superposition as a result of signal reflections from specimen edges

[5-7]. Thus, it is very challenging to achieve reliable damage identification using the conventional AE approaches based on the standard recorded AE data directly. Overcoming these intrinsic limitations will improve the reliability of the AE damage characterisation technique and provide much improved SHM capabilities.

Several studies have focussed on the use of AE to identify damage mechanisms in composite materials under different loading regimes. Clustering AE signals exhibiting similarities in to groups based on conventional AE analysis has been the main target of these studies by plotting traditional AE descriptors such as amplitude, count, duration, etc. versus load or number of cycles. The correlation between two or more AE descriptors using classification techniques, both unsupervised and supervised has also been investigated [1].

To discriminate between different damage mechanisms, some authors have correlated each damage type with frequency by using the peak frequency, time-frequency or frequency-intensity data from AE signals [8-18]. Others have correlated damage with a traditional AE parameter such as amplitude of AE signals [10, 15, 19-21]. However, the correlation between damage type and frequency range observed by different studies is dissimilar, suggesting that it is not a reliable approach to consider the frequency extracted from the AE waveforms as a discriminating factor. This is due to the fact that the frequency is dependent on many factors such as the structural geometry, sensor response, signal propagation path and source frequency [22]. Furthermore, using burst amplitude for damage classification in complex materials is often inaccurate [23].

In efforts to achieve greater reliability, many researchers have adopted multivariate approaches to signal classification. These multidimensional analyses consider a large number of AE signal descriptors in an attempt to provide a more powerful correlation between AE data from different damage mechanisms. Many multivariate classification approaches have been investigated both individually or in combination, these include algorithms such as k-means [24-29], k-Nearest Neighbours (k-NN)[27], Fuzzy c-means [30, 31], Principal Components Analysis (PCA) [25, 30], Gaussian mixture distribution (GMD) [26], Artificial Neural Network (ANN) (such as the Self-Organising Map (SOM) [26-29, 32-34] and Competitive Neural

Networks (CNN) [26]). These normally correlate the resultant classes with observable damage mechanisms and then use a single signal parameter such as the peak frequency or amplitude to validate the classification results. Most studies are conducted using signals received by a single sensor and recorded directly by an acquisition system without removing effects of propagation, which will likely affect the reliability of the classification result.

The objective of the present work is to use the AE technique to identify damage mechanisms generated within a large-scale laminated carbon fibre composite panel under low-cycle tension-tension fatigue. An AE parameter correction methodology known as the "Parameter Correction Technique (PCT)" [35, 36] is used to correct the propagation effects of AE data collected from the panel. An unsupervised classification technique, k-means, is then used to classify the AE data into suitable classes.

The PCT has been developed by the authors in order to correct for the propagation effects of as-recorded traditional AE parameters in large-scale composite structures with complex geometries. It has been previously demonstrated that this technique provides a reliable recalculation of the signal features recorded from artificial AE sources at different positions within a carbon fibre composite panel [36]. It is noteworthy that the PCT presents advantages over conventional techniques by overcoming the restriction of using data from a single sensor for analysis by utilising data from multiple sensors in the recalculation process for each signal parameter. Therefore no AE data is lost due to large source to sensor distances.

The work presented in this paper builds on two previous papers by the authors [36, 37] and shares the same experimental process. The initial paper focussing on PCT [36] used artificial data, created using a wave generator and a conical transducer, to demonstrate the technique. In [37], an Artificial Neural Network classifier was used on experimental AE data to explore approaches of self-learning to identify matrix cracking and delamination signals. This paper is the first recorded use of PCT to correlate real AE damage signals in composites that are validated by both ultrasonic scanning and CT scans. The Paper is arranged as follows. First an introduction to the PCT process and cluster analysis is given in Section 2. The experimental procedure is outlined in Section 3. In Section 4 a comparison between the traditional and re-calculated data classification is made and finally conclusions are drawn in Section 5.

2. Data Processing

The aim of this process is to cluster AE data into groups of similar signals using an unsupervised clustering technique. The differing classes identified will then be attributed to specific damage modes occurring during fatigue loading of a composite panel. It should be noted that it is the intention of the authors to apply this classification procedure to signals from located AE events only. That is, only AE sources with high energy which hit at least three sensors are considered as an event to be used in the analysis.

In this work four signal parameters, (Amplitude, Count, Duration and Energy), are used as input data in the clustering process. The classification procedure is performed twice, once using the traditional signal parameters and again using the re-calculated parameters from the PCT. Figure 1 presents an overview of the procedure adopted for analysing the AE signals. Each step will be described in this section (except assigning the results which will be discussed in Section 4).

2.1 Locate AE Events:

In anisotropic materials, such as composites, accurate AE location is complex due to variation in propagation velocity with direction. Some approaches have been taken to solving this problem [38-41] and improvements in accuracy have been shown in simple laminated plates. However none of these approaches account for structural complexities that may interrupt the wave propagation path, such as holes and thickness changes that may be present in an industrial environment. In order to overcome these obstacles Baxter et al. [42] presented the Delta T Mapping technique. This technique involves generating several artificial sources at each point on a grid defined across the structure and using the mean arrival time at each sensor to construct a map of arrival time difference for each pair of sensors. The maps are subsequently used in the location calculation and the technique has been demonstrated to provide superior location accuracy. Originally developed for complex geometry metallic structures [42], the technique has also been shown to perform very well in anisotropic materials such as composites [43]. Further improvements to this approach have been made by integrating an Akaike Information Criteria (AIC) based arrival time estimation [44] and automating training data cleaning and selection processes [45] which has significantly reduced operation time and increased reliability. The Delta T Mapping technique has been used to locate the AE events in this work.

2.2 AE Feature Correction:

In order to correct the traditional parameters of recorded AE signals the Parameter Correction Technique was performed. In this new technique a point contact, conical, piezoelectric transducer is used to excite artificial AE signals at locations across the structure of interest. The sources are excited at a range of amplitude levels and a multi-level map of feature variation with respect to source amplitude and spatial location is created. These maps are then used as the basis for feature correction based on accurately computed source location. A more detailed description of the PCT methodology can be found in previous work [35, 36]; however, a summary of the technique is provided below in five steps:

- **Determine area of interest**: The technique can provide complete coverage of a structure or part of a structure, it can be used as an improvement method to correct the signal parameters emitted from specific areas of expected fracture.
- **Construct grid system**: A grid is constructed on the area of interest within which AE events will be located. The parameter correction is performed with respect to the grid coordinates and not the sensor positions.
- **Obtain AE parameter value data set**: At each node of the grid, artificial sources with varying input amplitude are generated to provide AE parameter values at each sensor. An average result of the recorded AE data is achieved by repeating the same source amplitude several times at each node, to reduce error. Missing node data as a result of holes, for example, and the area between nodes are interpolated from the other surrounding data. The parameter values of each source amplitude within the grid will present a contour map.
- **Calculate PCT maps**: A multi-level (3D) map is then generated for each parameter by stacking up the individual contour maps. The layers are arranged, in order, from the lower source amplitude to the highest. From these maps, the relationship between the recorded parameter and the source amplitude will be calculated for each location.
- **Parameters re-calculation**: Using these AE parameter versus source amplitude relationships; the source amplitude for any previous, current or future AE data can be identified. To estimate the

parameter value of any event the average of all sensors used to locate that event will is used provide the most accurate value.

2.3 Traditional AE Features Normalisation

Before conducting the multivariable analysis a ‘prior normalisation” step was performed. In any multi-variable clustering process it is essential to normalise the data sets to ensure that each parameter has equal weighting to avoid biasing the solution towards the high parameter weightings. This step ensures that all data has been centred and reduced, posing a mean value equal to zero and a standard deviation equal to one. The difference between the solution of the normalised set and that of the original set will depend upon the extent to which the variance of the various parameters differ. This means that the results obtained from un-normalised data subjected to multi-dimensional analysis will be weighted in favour of the parameters with higher relative variance. When dealing with the traditional AE parameters, there is no acceptable reason to consider anything other than equal weighting and so the data presented to the classification technique were normalised. The normalisation step was conducted only with the traditional data because the re-calculated parameters naturally poses equal weighting.

2.4 Unsupervised Clustering and Cluster Quality Criteria

The two data sets, traditional and re-calculated, are then classified separately using *k*-means as an unsupervised clustering technique. The *k*-means method aims to minimize the sum of squared distance between all the vectors of a cluster and its centre [46]. In the *k*-means approach the number of clusters *k* should is specified in advance. In order to select the most appropriate value for *k*, two common clustering quality criterions, Silhouette [47] and Calinski-Harabasz [48] indexes, were used to determine the optimal number of classes which corresponding to the maximum value of the two criterions.

3. Experimental Procedure

3.1 Test specimen:

The carbon fibre specimen used in this investigation is shown in Figure 2. More details on the test specimen can be found in the work by Crivelli et al [37]. A 500 x 500 mm square panel was manufactured from 8 plies of Hexcel M21/35%/UD268/T800S uni-directional pre-preg material and cured in an autoclave in line with the manufacturers recommendations. A layup of $(0,90)_{2S}$ was used which resulted in a cured thickness of 2.1 mm. During layup a 25 mm cut, perpendicular to the fibres, was made at the centre of the two inner 0^o plies in order to promote matrix cracking under tensile load. Following manufacture the panel was inspected using ultrasonic C-scanning to ensure quality and uniformity.

In order to transfer the tension load to the test specimen, four 5mm thick aluminium tabs with 50 x 50 mm dimensions were glued on to both sides of the panel, along the 0^o material direction, using Araldite 420 (2 Component Epoxy Adhesive). To accelerate the gluing process the specimen with tabs were cured at 50 centigrade for 4 hours. A 20 mm diameter hole was drilled through each of the tabs to provide a load attachment point. After drilling the specimen was once again C-scanned in order to ensure that no internal damage had been induced. The specimen, when fitted in the test machine, as shown in Figure 2. Four 10 mm thick steel plates were used to extend the load machine clevis fixture down to the drilled holes and a 20 mm diameter bolt was placed through the extenders and the panel and tightened with a nut.

3.2 AE acquisition:

AE was continually monitored during the test using a Vallen AMSY-4 data acquisition system, with 5 MHz sample rate and 34 dB pre-amplification from Vallen AEP3 pre-amplifiers. The AE signals were monitored using five PAC WD wideband transducers. Ambient noise was filtered using a 44.9 dB threshold. The sensors were attached to the specimen using Silicon RTV (Loctite 595) to provide an acoustic couplant and a mechanical fixture. The relative positions of the sensors can be seen in Figure 3. The correct mounting of the sensors was verified by using the Hsu-Nielson (H-N) source [49].

A Delta T grid was created with two resolutions. A 300 x 300 mm grid with a 50 mm resolution was placed centrally on the panel (Figure 2 and 3a) and the central 100 x 100 mm area of the grid centred around the artificial crack was arranged with a 10 mm resolution. The training data for the Delta T Mapping technique was collected from this grid prior to the testing.

The PCT process utilised the same 300 x 300 mm grid, with a resolution of 50 mm that was used for the Delta T Mapping technique (Figure 2 and 3b). An artificial AE source was used to generate signals at each of the grid nodes to provide training data [36]. This was achieved by use of a Mistras Group Ltd. arbitrary waveform generator (WaveGen1410) and an in-house manufactured broadband conical transducer provided by the National Physical Laboratory, UK. Multi-purpose grease was used as a couplant to provide consistent acoustic transmission between the conical transducer and the specimen surface.

3.3 Test plan:

The tensile specimen was subjected to tension-tension fatigue load, with the maximum applied load increased from 8 to 31 kN throughout the test. The loading profile across the whole test is presented in Figure 4. After 130k cycles the panel was removed from the test rig and subjected to an impact. Subsequently the panel was returned to the test rig and loaded for an additional 155k cycles.

The test was performed in batches of 5k cycles at a rate of 1Hz. In order to follow the damage evolution, the specimen was inspected by ultrasonic C-scanning between the batches. The C-scan image and the AE activity were subsequently considered in order to decide whether to increase the load or run a further 5k cycle at the same load. The first part of Figure 4 (left of vertical dashed line) contains the batch numbers and the applied load before impact.

After 26 batches (130k cycles) of loading the panel was impacted at different energy levels (from 5 to 14 J) using an Instron Dynatup 9250HV impact test machine, to generate a new source of AE activity during the test. A C-scan inspection was performed following the impact testing. The panel was then subjected to further fatigue loading in line with the previous procedure. The second part of Figure 4 (right of vertical dashed line) shows the applied load for batches of cycles after impact. At the end of the test, the panel was C-scanned for a final time and then a ~50 x 200 mm section centred on the cut plies was removed for x-ray CT evaluation, to verify the development of matrix cracking local to the cut ply region.

4. Results and discussion

4.1 Physical observations

The C-scan images are shown in Figure 5 and reveal the different conditions of the panel during the test. After manufacturing, the C-scan image shows there is no internal damage (Figure 5a). After applying the first 26 loading batches (ending with 21 kN load after 130k cycles) the panel is still without any signs of internal damage (Figure 5b). The artificial crack location indicates a very slightly higher attenuation, but it is difficult to identify in-plane cracking by C-scan inspection so this cannot be considered conclusive. After impact (Figure 5c), a clear region of high attenuation is observed just above the lower tab indicating the location of impact induced delamination. The dark spot seen centrally in all the images is sensor 5 with its cable exiting to the left of the image also visible. At the end of the test (31 kN load after 285k cycles) no discernible growth in the delamination area can be observed, suggesting that the delamination has not grown during the test (Figure 5d). Again a mild increase in attenuation at the cut plies (just below sensor 5) is observable in Figure 5d but no positive indication of matrix crack growth can be inferred from this.

The CT scan results are shown in Figure 6 which show the final condition of the cut ply region after the test. The figure shows two selected slices which corresponding to the third ply depth (Figure 6a) and the sixth ply depth (Figure 6b), i.e. the depth of the cut plies. The main images (1) show an in-plane slice through the material at the stated depth and the two additional images (2 & 3) show orthogonal through thickness slices at the same location. The red arrows indicate a common position that is collocated within all three images. A clear horizontal crack like feature is seen running horizontally left to right in both main images, these cracks correspond to the cut ply positions with in the sample. The through thickness slices (2) show corresponding indication of cracking at these positions, appearing as a small black dot because the crack is running out of the plane of the page. Image 3 at a depth of 3 plies also shows a clear indication of cracking. At a depth of 6 plies the crack is less obvious in image 3, suggesting that the crack is less well developed at this depth. By comparing image 2 from both Figure 6 a) and b) it can be seen that the cut plies are miss-aligned and this miss-alignment has restricted the growth of a larger through thickness matrix crack. The CT results, however, confirm that matrix cracking has occurred at the resin rich pockets made at the position of the cut fibres in the laminate.

The Delta T results for AE source location using all the five sensors are shown in Figure 7 a) and b) for before and after impact, respectively. In Figure 7a, before impact, events are clustered close to the tab boundaries and at the central area of the specimen at the location of the cut plies. Figure 7b, post impact, shows the events located from the final loading batch (31). High AE activity is observed at the upper tab location with very little activity observed at the lower tab. A cluster of events is also observed at the location of the impact induced delamination. Additionally, some AE events are located in the unloaded area to the left of the presented image and these events are assumed to be miss-located. Some miss-located events is common in AE testing and often occurs from low amplitude signals where accurate arrival time determination is difficult. The percentage of miss-located events (e.g. x=<10) is ~6.6% of the total located events in this data set and therefore these events are not deemed to be significant. These results demonstrate that the Delta T Mapping approach is able to accurately detect and locate signals from noise sources, such as the tabs, and from differing damage mechanisms, such as the matrix cracking and delamination. However to gauge the significance of any located events in a realistic monitoring situation an indication of the source mechanism is required, i.e. signal classification is needed.

In order to perform damage identification this work focuses on the signals located at the artificial cracking and delamination areas only. The located events before impact were selected for the clustering purpose limited on the area of artificial crack (the selected signals presented in Figure 7a). Figure 7b, post impact, presents the selected signals from both the delamination and artificial crack areas.

Figure 8 presents the percentage of events for which a sensor was not used in the location calculation, that is the number of events or signals that would be missed if each sensor was considered in isolation. Counter-intuitively; being closest to the damage region, channel 5 is missing signals for over 22% of the events located. When the total number of hits at each channel are considered channel 5 has recorded significantly more than all other channels with a large number of low energy signals that are not registered by sensors further away due to attenuation. This disparity is attributed to the process used for the Delta T Mapping algorithm to group signals closely spaced in time that will likely be from the same event. It is anticipated that the large number of additional hits on channel 5 has caused some errors in correct identification of event groups. Nevertheless, Figure 8 serves to highlight the issue of data loss when only one sensor is considered for classification. Here it would be most intuitive to select channel 5, however that would result in the loss of 22.6% of all located events when all 5 sensors are considered. The PCT technique overcomes this limitation by using corrected data from all sensors to provide an average corrected feature value. So, all data from located events can be considered in any subsequent classification work, which is an important advantage for improving the performance and reliability of AE damage classification in large-scale components.

4.2 AE data classification

The proposed classification approach was performed for two cases: 1) using traditional AE parameters and 2) PCT corrected AE parameters. The input vector to the classifier in each case is the same four signal features (Amplitude, Energy, Count and Duration). After normalising the traditional features recorded using each one of the five sensors and recalculating the AE parameters using the PCT, the optimal number of classes was calculated for each of the six data sets, according to the two clustering quality criteria discussed above. Then the six data sets were classified using these optimum cluster numbers. The number of events allocated to each class, following classification, is presented in Figure 9 as a percentage of the total number of events recorded by the used sensor. The use of traditional parameters leads to more than one solution that mainly depends on the sensor from which data was used as input to the classifier. Thus it is difficult to decide which result is correct. Normally the operator will select the result from the sensor with the largest data quantity or the result which corresponds to any expected damage. On the other hand, there is one single solution arising from the use of data corrected by the PCT approach, which reduces uncertainty and avoids the need for operator decisions within the analysis.

Practically, it is difficult to rely on data from one sensor to achieve reliable damage classification when the AE sources are located at different distances from the sensor [36]. Furthermore, in general using data from one sensor leads to the loss of some located AE data which will have a negative effect on classification reliability. The PCT approach has previously demonstrated the ability to overcome these limitations for artificial AE sources [36]. Here further analysis of its ability to accurately classify different damages mechanisms from fatigue test data is made.

In order to characterise the possible damage mechanisms occurring in this test, the AE data is divided into two parts: the pre-impact stage which corresponds to the located AE activity at the artificial crack region (Figure 7a) and the post-impact stage which corresponding to the activity at both damage regions, i.e. artificial crack and delamination area (Figure 7b).

In the pre-impact stage the cut plies are located in the load path between the two aluminium tabs, where it is expected that the stress will be sufficient to cause cracking in the resin pocket between cut fibres. The x-ray CT data presented in Figure 6 confirms the growth of matrix cracking in this region. Hence there is high confidence that the AE signals selected from the crack region were generated from the observed matrix cracking damage. After the initial AE activity in the cut ply region, no further AE data was observed in this region. This is due to the developed cracks reaching the end of the cut ply region and being arrested by the intact continuous fibres. When plotting the location of the PCT classes as two segments, before and after impact, as shown in Figure 10 it can be seen that prior to impact Class-2 is the dominant class. Hence it is concluded that Class-2 results from the matrix cracking damage mechanism.

The post impact stage contains events mostly located in the region of the delamination, with a small number of events located near the cut ply region, indicating that some additional matrix cracking might have been induced by the higher applied load of 31kN (Figure 10). Significant activity is seen in the delamination region, despite the C-scan data showing no obvious signs of delamination growth. The AE activity in this region is likely to result from a range of sources including matrix cracking caused by the induced stress concentrations and friction from fretting and movement of the existing damage surfaces. For the data recorded after impact the PCT classification identifies two classes (Figure 10). The signals located at the delamination site are a mixture of class 1 and 2, which is expected due to the varied damage mechanisms present in this area, with class 2 representing matrix cracking and class 1 representing fretting of the delamination surfaces. Out of the small number of signals located near the crack most are class 2 and located in the region of the crack tips and correspond to the observed matrix cracking.

The presented methodology provides a solution to the challenges of AE signal classification in large-scale structures, by eliminating signal propagation effects. The PCT provided a single classification solution, while use of traditional features leads to multiple ambiguous solutions, depending on the sensor selected. It has also been shown that data from all sensors is utilised in the PCT process, thus eliminating the potential loss of some located events. This work has demonstrated that the developed methodology allows AE signals from different sources to be reliably classified into separate groups. The classification result achieved using the data corrected by the PCT provide a more reliable solution. Two classes corresponding to matrix cracking and fretting signals were detected, located and classified. Currently the PCT cannot be directly implemented in true real time, however, development of a real time implementation of the presented technique will form the focus of further work.

5. Conclusions:

The main aim of the present work is to use the AE data recorded from the fatigue test of a composite material panel to identify different source mechanisms. The Delta T and PCT techniques were used to locate the AE events and correct AE features with high performance. The resulting clusters clearly identify the most critical damage types. The C-scan and CT scan results support the proposition that the AE technique can detect two different damage mechanisms and these are most likely to be matrix cracking and delamination movement.

The PCT is shown to be an effective tool to correct signal features and overcome the propagation path influence on the recorded AE data. Furthermore using data from multiple sensors enables all the located events to be accounted for in the final analysis without loss of data.

Acknowledgements

The authors would like to thank the Iraqi Ministry of Higher Education and Scientific Research for supporting this research and the technical staff of Cardiff University School of Engineering for their kind assistance with the testing programme.

References

[1] Miller KR, Hill EK. Nondestructive Testing Handbook, Acoustic Emission Testing. 3rd ed2005.

[2] Sause MGR, Müller T, Horoschenkoff A, Horn S. Quantification of Failure Mechanisms in Mode-I Loading of Fiber Reinforced Plastics Utilizing Acoustic Emission Analysis. Composites Science and Technology. 2012;72(2):167-74.

[3] Maillet E, Godin N, R'Mili M, Reynaud P, Fantozzi G, Lamon J. Damage monitoring and identification in SiC/SiC minicomposites using combined acousto-ultrasonics and acoustic emission. Composites Part A: Applied Science and Manufacturing. 2014;57:8-15.

[4] Dzenis YA. Cycle-based analysis of damage and failure in advanced composites under fatigue: 1. Experimental observation of damage development within loading cycles. International Journal of Fatigue. 2003;25(6):499-510.

[5] W. H. Prosser KEJ, S. Kellas, B. T. Smith, J. McKeon, and A. Friedman. Advanced, Waveform Based Acoustic Emission Detection of Matrix Cracking in Composites. Materials Evaluation. 1995;53(9):1052-8.

[6] Moevus M, Rouby D, Godin N, R'Mili M, Reynaud P, Fantozzi G, et al. Analysis of Damage Mechanisms and Associated Acoustic Emission in Two Sic/[Si–B–C] Composites Exhibiting Different Tensile Behaviours. Part I: Damage Patterns and Acoustic Emission Activity. Composites Science and Technology. 2008;68(6):1250-7.

[7] Johnson M. Waveform Based Clustering and Classification of AE Transients in Composite Laminates Using Principal Component Analysis. NDT & E International. 2002;35(6):367-76.

[8] Kinjo T, Suzuki H, Saito N, Takemoto M, Ono K. Fracture-mode classification using wavelet-transformed AE signals from a composite. Journal of acoustic emission. 1997;15(1-4):19-32.

[9] Mäder E, Moos E, Karger-Kocsis J. Role of film formers in glass fibre reinforced polypropylene — new insights and relation to mechanical properties. Composites Part A: Applied Science and Manufacturing. 2001;32(5):631-9.

[10] Morscher GN. Modal acoustic emission of damage accumulation in a woven SiC/SiC composite. Composites Science and Technology. 1999;59(5):687-97.

[11] Loutas TH, Kostopoulos V, Ramirez-Jimenez C, Pharaoh M. Damage evolution in center-holed glass/polyester composites under quasi-static loading using time/frequency analysis of acoustic emission monitored waveforms. Composites Science and Technology. 2006;66(10):1366-75.

[12] de Groot P, Wijnen P, Janssen R. Real-Time Frequency Determination of Acoustic Emission for Different Fracture Mechanisms in Carbon/Epoxy Composites. Composites Science and Technology. 1995;55(4):405-12.

[13] Woo SC, Choi NS, Cho N. Characterization of the Fracture Process of Notched Glass Fiber/Aluminum Hybrid Laminates by Acoustic Emission. Composites Science and Technology. 2008;68(6):1521-30.

[14] Oskouei AR, Ahmadi M, Hajikhani M. Wavelet-based acoustic emission characterization of damage mechanism in composite materials under mode Idelamination at different interfaces. eXPRESS Polymer Letters. 2009;3(12):804-13.

[15] Li L, Lomov SV, Yan X. Correlation of acoustic emission with optically observed damage in a glass/epoxy woven laminate under tensile loading. Composite Structures. 2015;123:45-53.

[16] Ni QQ, Iwamoto M. Wavelet transform of acoustic emission signals in failure of model composites. Engineering Fracture Mechanics. 2002;69(6):717-28.

[17] Ramirez-Jimenez CR, Papadakis N, Reynolds N, Gan TH, Purnell P, Pharaoh M. Identification of Failure Modes in Glass/Polypropylene Composites by Means of the Primary Frequency Content of the Acoustic Emission Event. Composites Science and Technology. 2004;64(12):1819-27.

[18] Qi G. Wavelet-Based AE Characterization of Composite Materials. NDT & E International. 2000;33(3):133-44.

[19] Kim ST, Lee YT. Characteristics of damage and fracture process of carbon fiber reinforced plastic under loading-unloading test by using AE method. Materials Science and Engineering: A. 1997;234:322-6.

[20] Kotsikos G, Evans JT, Gibson AG, Hale J. Use of acoustic emission to characterize corrosion fatigue damage accumulation in glass fiber reinforced polyester laminates. Polymer Composites. 1999;20(5):689-96.

[21] Liu PF, Chu JK, Liu YL, Zheng JY. A Study on the Failure Mechanisms of Carbon Fiber/Epoxy Composite Laminates Using Acoustic Emission. Materials & Design. 2012;37:228-35.

[22] Eaton MJ, Holford, Karen Margaret, Featherston, Carol Ann and Pullin, Rhys. Damage in Carbon Fibre Composites: The Discrimination of Acoustic Emission Signals Using Frequency. Journal of Acoustic Emission. 2007;25 140-8.

[23] Bravo A, Toubal L, Koffi D, Erchiqui F. Characterization of tensile damage for a short birch fiber-reinforced polyethylene composite with acoustic emission. International Journal of Material Science. 2013;3(3):79-89.

[24] Momon S, Godin N, Reynaud P, R'Mili M, Fantozzi G. Unsupervised and Supervised Classification of AE Data Collected During Fatigue Test on CMC at High Temperature. Composites Part A: Applied Science and Manufacturing. 2012;43(2):254-60.

[25] Li L, Lomov SV, Yan X, Carvelli V. Cluster analysis of acoustic emission signals for 2D and 3D woven glass/epoxy composites. Composite Structures. 2014;116:286-99.

[26] Sawan HA, Walter ME, Marquette B. Unsupervised learning for classification of acoustic emission events from tensile and bending experiments with open-hole carbon fiber composite samples. Composites Science and Technology. 2015;107:89-97.

[27] Godin N, Huguet S, Gaertner R, Salmon L. Clustering of Acoustic Emission Signals Collected During Tensile Tests on Unidirectional Glass/Polyester Composite Using Supervised and Unsupervised Classifiers. NDT & E International. 2004;37(4):253-64.

[28] Godin N, Huguet S, Gaertner R. Integration of the Kohonen's self-organising map and k-means algorithm for the segmentation of the AE data collected during tensile tests on cross-ply composites. NDT & E International. 2005;38(4):299-309.

[29] de Oliveira R, Marques AT. Health monitoring of FRP using acoustic emission and artificial neural networks. Computers & Structures. 2008;86(3):367-73.

[30] Oskouei AR, Heidary H, Ahmadi M, Farajpur M. Unsupervised Acoustic Emission Data Clustering For the Analysis of Damage Mechanisms in Glass/Polyester Composites. Materials & Design. 2012;37:416-22.

[31] Marec A, Thomas JH, El Guerjouma R. Damage Characterization of Polymer-Based Composite Materials: Multivariable Analysis and Wavelet Transform For Clustering Acoustic Emission Data. Mechanical Systems and Signal Processing. 2008;22(6):1441-64.

[32] Gutkin R, Green CJ, Vangrattanachai S, Pinho ST, Robinson P, Curtis PT. On acoustic emission for failure investigation in CFRP: Pattern recognition and peak frequency analyses. Mechanical Systems and Signal Processing. 2011;25(4):1393-407.

[33] Albouy W, Vieille B. Determination of the damage threshold in woven-ply thermoplastic laminates at T > Tg : Acoustic emission and microscopic damage analysis. Composites Part B: Engineering. 2014;64:138-46.

[34] Crivelli D, Guagliano M, Monici A. Development of an artificial neural network processing technique for the analysis of damage evolution in pultruded composites with acoustic emission. Composites Part B: Engineering. 2014;56:948-59.

[35] Al-Jumaili SK, Holford KM, Pullin R, Eaton MJ. A Parameter Correction Technique (PCT) for Acoustic Emission Characterisation in Large-Scale Composites. In: Proceedings of 31st Conference of the European Working Group on Acoustic Emission (EWGAE). Dresden, Germany, Conference, Conference 2014.

[36] Al-Jumaili SK, Holford KM, Eaton MJ, Pullin R. Parameter Correction Technique (PCT): A novel method for acoustic emission characterisation in large-scale composites. Composites Part B: Engineering. 2015;75:336-44.

[37] Crivelli D, Guagliano M, Eaton M, Pearson M, Al-Jumaili S, Holford K, et al. Localisation and identification of fatigue matrix cracking and delamination in a carbon fibre panel by acoustic emission. Composites Part B: Engineering. 2015;74:1-12.

[38] Ciampa F, Meo M. A new algorithm for acoustic emission localization and flexural group velocity determination in anisotropic structures. Composites Part A: Applied Science and Manufacturing. 2010;41(12):1777-86.

[39] Kundu T, Nakatani H, Takeda N. Acoustic source localization in anisotropic plates. Ultrasonics. 2012;52(6):740-6.

[40] Niri DE, Farhidzadeh A, Salamone S. Nonlinear Kalman Filtering for acoustic emission source localization in anisotropic panels. Ultrasonics. 2014;54(2):486-501.

[41] Kundu T, Yang X, Nakatani H, Takeda N. A two-step hybrid technique for accurately localizing acoustic source in anisotropic structures without knowing their material properties. Ultrasonics. 2015;56:271-8.

[42] Baxter MG, Pullin R, Holford KM, Evans SL. Delta T Source Location for Acoustic Emission. Mechanical Systems and Signal Processing. 2007;21(3):1512-20.

[43] Eaton MJ, Pullin R, Holford KM. Acoustic Emission Source Location in Composite Materials Using Delta T Mapping. Composites Part A: Applied Science and Manufacturing. 2012;43(6):856-63.

[44] Pearson MR, Eaton M, Featherston C, Pullin R, Holford K. Improved acoustic emission source location during fatigue and impact events in metallic and composite structures. Structural Health Monitoring. 2016;1:18.

[45] Al-Jumaili SK, Pearson MR, Holford KM, Eaton MJ, Pullin R. Acoustic emission source location in complex structures using full automatic delta T mapping technique. Mechanical Systems and Signal Processing. 2016;72–73:513-24.

[46] MacQueen J. Some Methods for Classification and Analysis of Multivariate Observations. In: Proceedings of the fifth Berkeley symposium on mathematical statistics and probability. Conference, Conference 1967. p. 281-97.

[47] Rousseeuw PJ. Silhouettes: A Graphical Aid to the Interpretation and Validation of Cluster Analysis. Journal of Computational and Applied Mathematics. 1987;20:53-65.

[48] Dudoit S, Fridlyand J. A prediction-based resampling method for estimating the number of clusters in a dataset. Genome Biology. 2002;3(7):1-21.

[49] Hsu NN, Breckenridge FR. Characterization and Calibration of Acoustic Emission Sensors. Materials Evaluation. 1981;39(1):60-8.

Figure Captions

Figure 1. Flow chart representation of the methodology proposed in the analysis.

Figure 2. The specimen fitted in the tensile machine [37].

Figure 3. Sensors locations and (a) Delta T grid (b) PCT grid.

Figure 4. Test plan with the applied load per batch.

Figure 5. The C-scan result during the test (a) After manufacturing, before apply the load (b) Before impact, after batch number 26 (c) After impact immediately (d) After impact, After batch number 31.

Figure 6. The CT scan result at the end of the test a) 3rd ply depth and b) 6th ply depth.

Figure 7. The Delta T location of the recorded events (a) before impact (b) after impact.

Figure 8. Located events losing depend on the used sensor.

Figure 9. The Classes percentage for each case.

Figure 10. Delta T Mapping locations of the classification results (PCT).

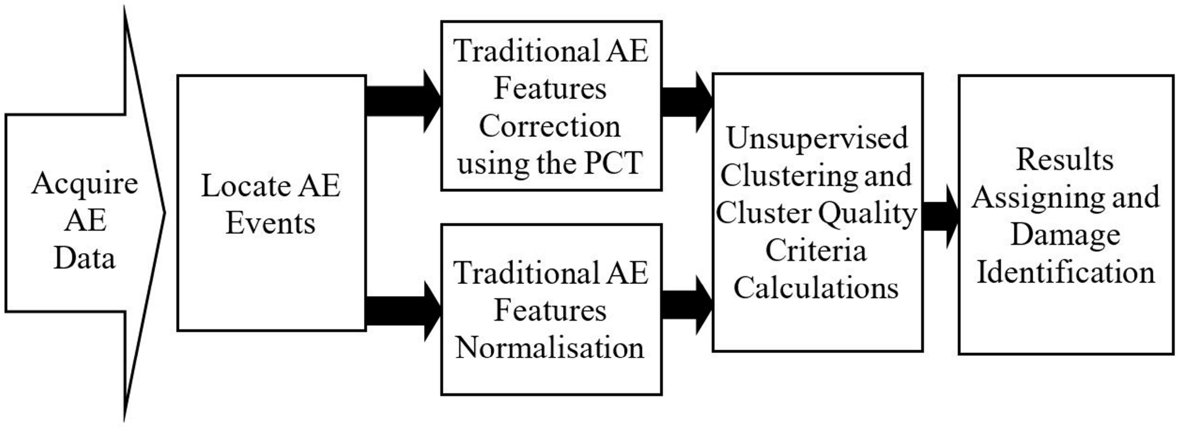
Acquire AE Data
Locate AE Events
Traditional AE Features Correction using the PCT
Traditional AE Features Normalisation
Unsupervised Clustering and Cluster Quality Criteria Calculations
Results Assigning and Damage Identification

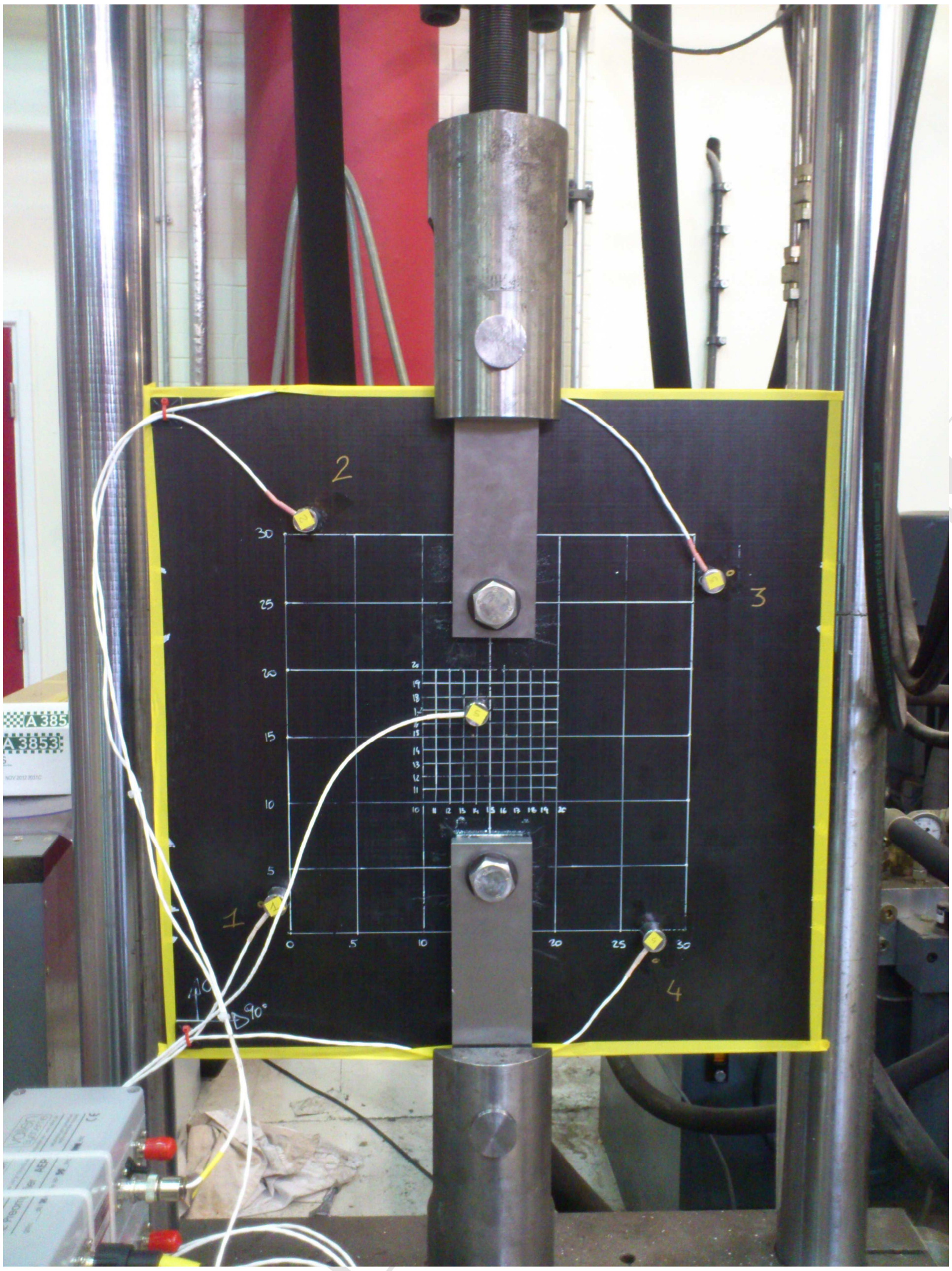

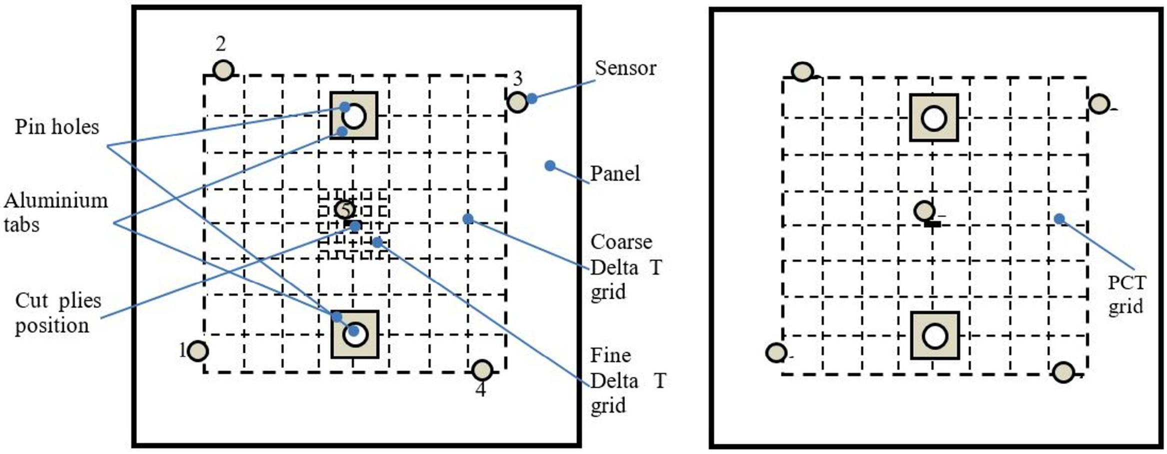

2
3
Sensor
Pin holes
Panel
Aluminium tabs
Coarse Delta T grid
Cut plies position
1
4
Fine Delta T grid
PCT grid

(a)

(b)

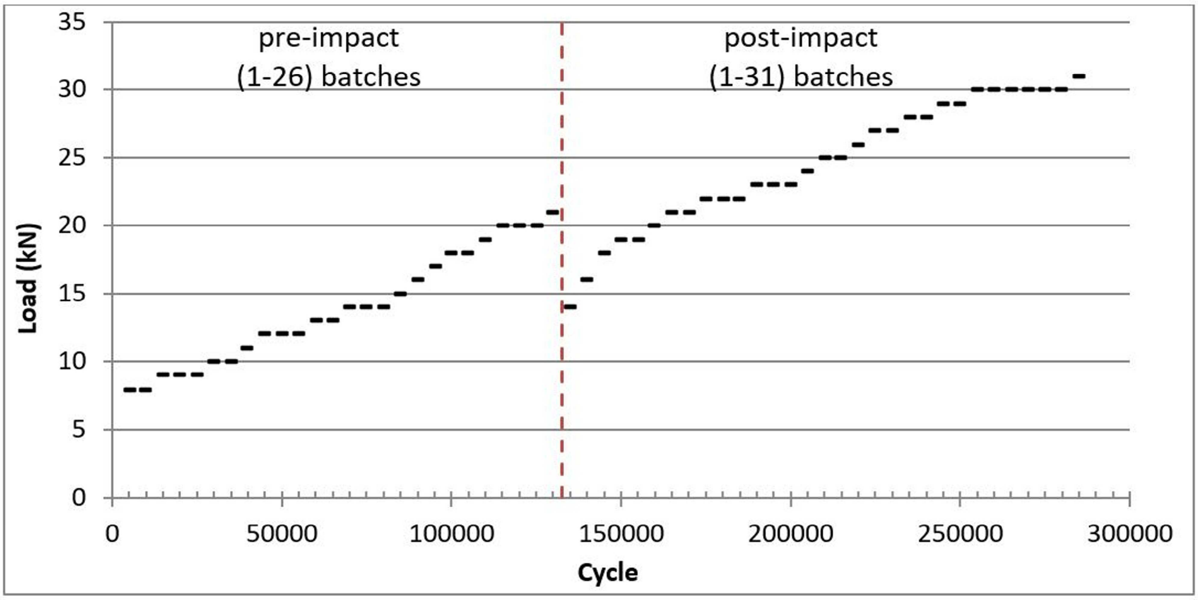

pre-impact
(1-26) batches
post-impact
(1-31) batches
Load (kN)
Cycle
0
5
10
15
20
25
30
35
0
50000
100000
150000
200000
250000
300000

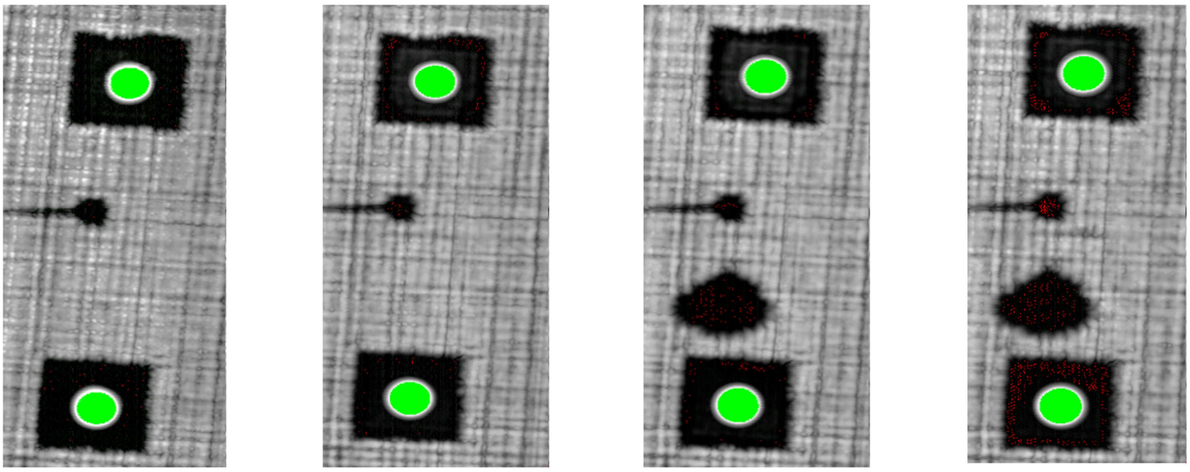

(a) (b) (c) (d)

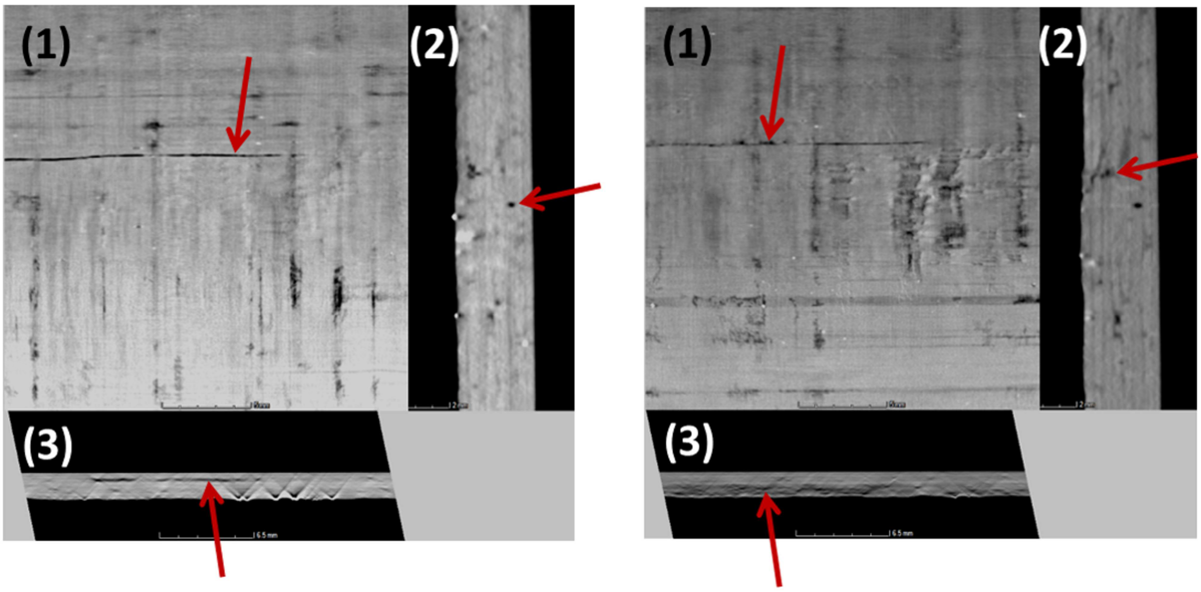

(a) (b)

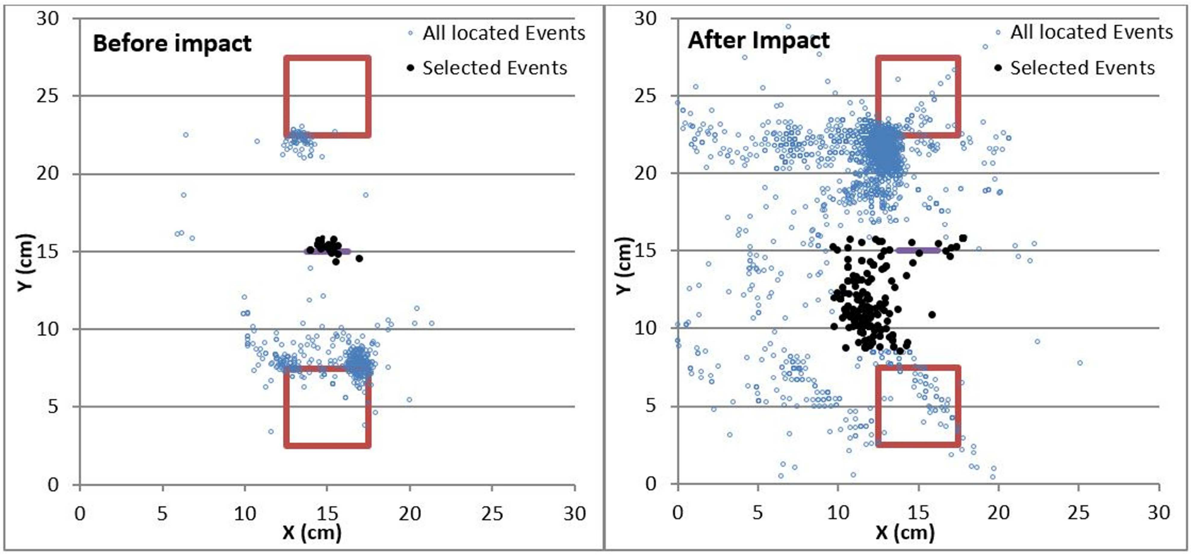
Before impact
All located Events
Selected Events
Y (cm)
X (cm)
After Impact
All located Events
Selected Events
Y (cm)
X (cm)

(a) (b)

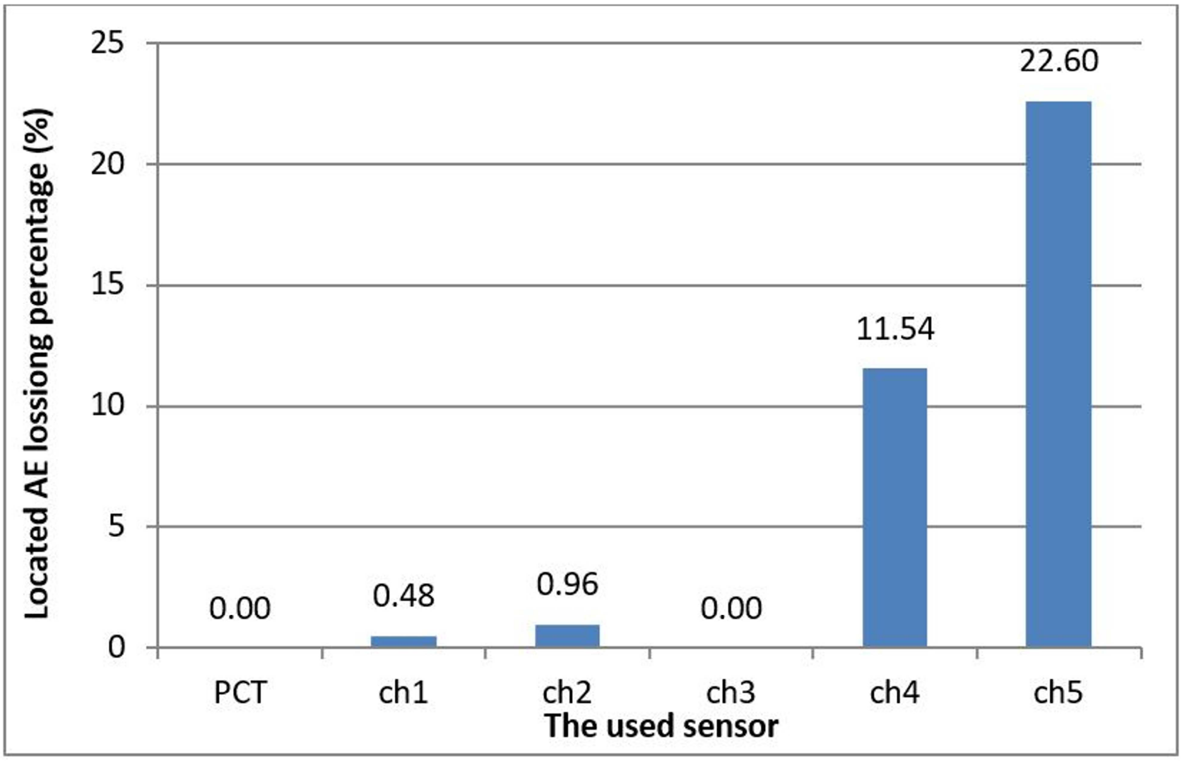
25
20
15
10
5
0
Located AE lossiong percentage (%)
0.00
0.48
0.96
0.00
11.54
22.60
PCT
ch1
ch2
ch3
ch4
ch5
The used sensor

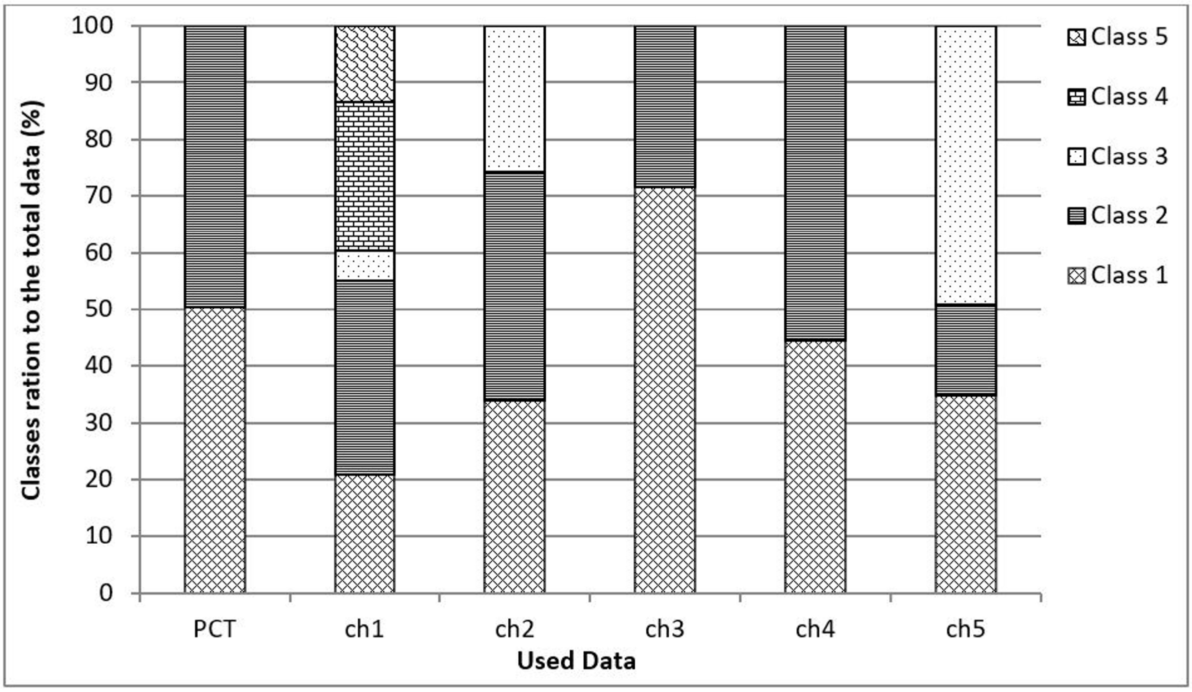
Class 5
Class 4
Class 3
Class 2
Class 1
Classes ration to the total data (%)
0
10
20
30
40
50
60
70
80
90
100
PCT
ch1
ch2
ch3
ch4
ch5
Used Data

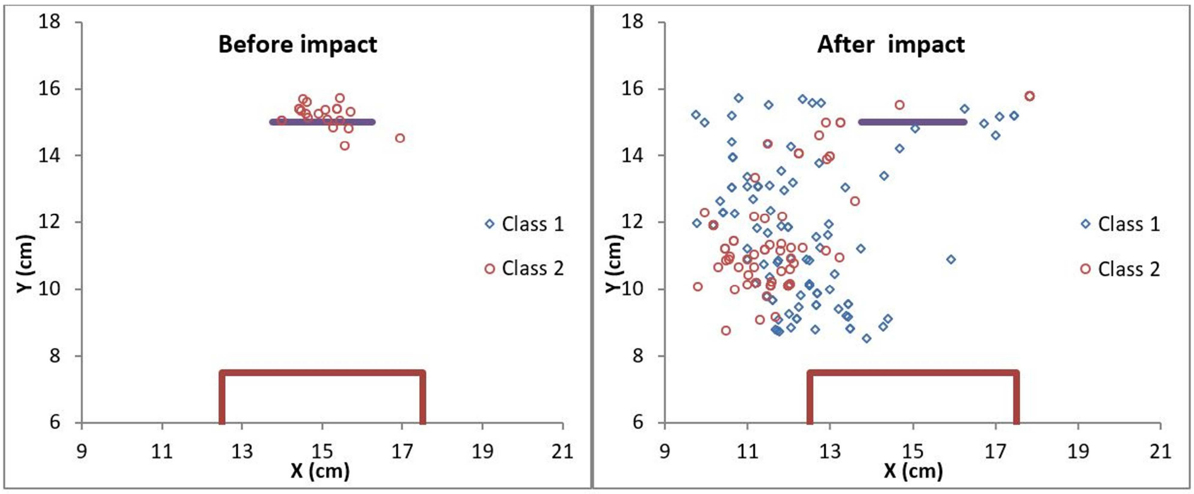
Before impact
After impact
Class 1
Class 2
Y (cm)
X (cm)